

The key physical parameters governing frictional dissipation in a precipitating atmosphere

A. M. MAKARIEVA, V. G. GORSHKOV, A. V. NEFIODOV

Theoretical Physics Division, Petersburg Nuclear Physics Institute, 188300, Gatchina, St. Petersburg, Russia

D. SHEIL*

School of Environmental Science and Management, Southern Cross University, PO Box 157, Lismore, NSW 2480, Australia

Institute of Tropical Forest Conservation, Mbarara University of Science and Technology, PO Box, 44, Kabale, Uganda

Center for International Forestry Research, PO Box 0113 BOCBD, Bogor 16000, Indonesia

A. D. NOBRE

Centro de Ciência do Sistema Terrestre INPE, São José dos Campos SP 12227-010, Brazil

P. BUNYARD

Lawellen Farm, Withiel, Bodmin, Cornwall, PL30 5NW, United Kingdom and University Sergio Arboleda, Bogota, Colombia

B.-L. LI

XIEG-UCR International Center for Arid Land Ecology, University of California, Riverside, USA

arXiv:1208.3734v2 [physics.ao-ph] 21 Aug 2012

ABSTRACT

Precipitation generates small-scale turbulent air flows the energy of which ultimately dissipates to heat. The power of this process has previously been estimated to be around 2-4 W m^{-2} in the tropics: a value comparable in magnitude to the dynamic power of the global circulation. Here we suggest that this previous power estimate is approximately double the true figure. Our result reflects a revised evaluation of the mean precipitation path length H_P . We investigate the dependence of H_P on surface temperature, relative humidity, temperature lapse rate and degree of condensation in the ascending air. We find that the degree of condensation, defined as the relative change of the saturated water vapor mixing ratio in the region of condensation, is a major factor determining H_P . We estimate from theory that the mean large-scale rate of frictional dissipation associated with total precipitation in the tropics lies between 1 and 2 W m^{-2} and show that our estimate is supported by empirical evidence. We show that under terrestrial conditions frictional dissipation constitutes a minor fraction of the dynamic power of condensation-induced atmospheric circulation, which is estimated to be at least 2.5 times larger. However, because H_P increases with surface temperature T_s , the rate of frictional dissipation would exceed that of condensation-induced dynamics, and thus block major circulation, at $T_s \gtrsim 320$ K in a moist adiabatic atmosphere.

* *Corresponding author.*

1. Introduction

Understanding the physics of a moist atmosphere and capturing it in theoretical concepts is a major challenge for climate science (Schneider 2006; Schiermeier 2010; Cotton et al. 2011). Among the complications introduced by water vapour are the various influences of precipitation on atmospheric motion. One specific aspect is that precipitation generates small-scale air turbulence around the falling condensate particles. The energy for this turbulent air motion derives from the potential energy of the rain drops or ice particles (i.e. "hydrometeors") in the gravitational field of Earth and is ultimately dissipated to heat. If this energy were not converted to turbulent kinetic energy of the air, the hydrometeors would continue to accelerate as they fall. But air exerts a drag force that prevents this acceleration. This force grows with increasing size of the hydrometeor and its velocity W relative to the surrounding air. Thus, as the condensate particle is accelerated by gravity, this opposing force grows until it equals the weight of the particle. Acceleration ceases at this resulting terminal velocity W_t . Since hydrometeors fall at near their terminal velocities for most of the duration of their falls, the mean drag force acting on them over this period is approximately equal to their weight.

Consider a column of moist air as a mixture of dry air and water vapor which we denote here using subscripts d and v respectively, standing for dry air and water vapor. In hydrostatic equilibrium,

$$-\frac{\partial p}{\partial z} = \rho g, \tag{1}$$

where $p = p_d + p_v$ is air pressure, $\rho = \rho_d + \rho_v$ is air density, g is the acceleration of gravity. There is no available potential energy in such a column. We now cool this column

in such a manner that some water vapor condenses. Two types of potential energy have now become available: the potential energy of droplets in the gravitational field and the potential energy of any non-equilibrium air pressure gradient that may have formed upon condensation. We recently proposed that the release of the second type of potential energy, i.e. that associated with the non-equilibrium gradient of saturated water vapor, is a major driver of atmospheric circulation on Earth (Makarieva and Gorshkov 2007; Makarieva et al. 2010; Gorshkov et al. 2012). Since precipitation and, hence, frictional dissipation of the potential energy of hydrometeors, always accompany condensation, it is important to estimate and contrast the power of the two processes in order to understand their relative influences.

In this paper we first examine how the power D of precipitation-related frictional dissipation can be estimated from basic atmospheric parameters. We then compare our results to those of Pauluis et al. (2000) and explain why our estimates are more consistent with both theory and data. We also discuss why the recent estimate of D by Pauluis and Dias (2012) from satellite-derived tropical rain rates does not constrain the true value more accurately than our theoretical analysis. We show that D grows with increasing surface temperature and estimate the critical temperature when the power of frictional dissipation equals the power of condensation-induced dynamics, such that the latter ceases.

2. Basic formulae

The power of dissipation of energy D (W m^{-2}) per unit area associated with small-scale turbulence around hydrometeors can be written as

$$D = \int_0^\infty W F_c dz = \int_0^\infty W_t g \rho_c dz. \quad (2)$$

Here $W \equiv w_c - w > 0$ is the mean velocity of hydrometeors relative to the air, w_c and w are the vertical velocities of condensate particles and air relative to the Earth's surface, F_c is the turbulent drag force per unit air volume exerted by air on hydrometeors, $\rho_c = N_c m$ is condensate density, N_c is the number of hydrometeors per unit volume and m is their mean mass. The second equality in (2) takes into account our assumption that hydrometeors are falling at their terminal velocity W_t , such that the drag force acting on a droplet is equal to its weight. For a constant W_t Eq. (2) simply represents the product of $W_t g$ and the total amount of condensate in the atmospheric column.

Equation (2) is not suited for a theoretical analysis. The distribution of W_t , which depends strongly on particle size, is poorly known. The amount of condensate in the atmosphere varies greatly in time and space, from a few kilograms per square meter in severe storms to less than a hundred grams per square meter under normal conditions (e.g., Jiang et al. 2008; Wood et al. 2002). Nonetheless, as we shall now show, it is possible to modify Eq. (2) to exclude these uncertain parameters.

Let us first consider the case when the terminal velocity of hydrometeors is much larger than air velocity, $W_t \gg |w|$. Neglecting for now re-evaporation of condensate in the column we assume that all condensate that has formed in the course of the ascent of moist air

precipitates to the ground. In such a case the power D becomes

$$D = \rho_{cs}W_{ts}gH_P = P_s gH_P. \quad (3)$$

Here ρ_{cs} and W_{ts} are respectively the condensate density and the terminal velocity of hydrometeors near the ground surface, precipitation path length H_P is the mean height from which the hydrometeors are falling, $P_s = \rho_{cs}W_{ts}$ is precipitation measured at the surface in $\text{kg H}_2\text{O m}^{-2} \text{ s}^{-1}$. When a hydrometeor falls to the ground from height H_P , the potential energy that it has lost per unit mass is gH_P . Precipitation P_s tells us how much water hits the ground per unit surface area per unit time, so $D = P_s gH_P$ gives the total rate of potential energy loss by all hydrometeors in the column.

At $W_t \gg |w|$ there is no upward transport of condensate that originated in the lower atmospheric layers: the hydrometeors fall to the ground from where they were formed. Rate of condensation S ($\text{mol H}_2\text{O m}^{-3} \text{ s}^{-1}$) in the ascending air is equal to

$$S = -w \left(\frac{\partial N_v}{\partial z} - \gamma \frac{\partial N}{\partial z} \right) \equiv -wN \frac{\partial \gamma}{\partial z} > 0, \quad \gamma \equiv \frac{N_v}{N} = \frac{p_v}{p}, \quad (4)$$

where N_v and N are the molar densities of water vapor and air (Makarieva et al. 2010; Gorshkov et al. 2012). The value of S differs from zero only in a certain area $z_1 \leq z \leq z_2$, where the relative humidity is close to unity and the water vapor is saturated. Precipitation path length H_P is then equal to the mean height of condensation:

$$H_P = \frac{\int_0^\infty S(z)z dz}{\int_0^\infty S(z) dz} = \frac{\gamma^*(z_1)z_1 - \gamma^*(z_2)z_2 + \int_{z_1}^{z_2} \gamma^*(z) dz}{\gamma^*(z_1) - \gamma^*(z_2)}. \quad (5)$$

Here z_1 and z_2 are the heights of the lower and upper boundaries of the condensation area ($S = 0$ at $z < z_1$ and $z > z_2$), $\gamma = \gamma^* \equiv p_v^*/p$ is equal to the ratio of saturated water

vapor partial pressure p_v^* to air pressure p . (Note that $\gamma^* = (M_d/M_v)q^*/[1 + q^*(M_d/M_v)] \simeq (M_d/M_v)q^*$, where $q^* \equiv \rho_v^*/\rho_d$ is the saturated water vapor mixing ratio, M_v and M_d are the molar masses of the water vapor and dry air, respectively. Thus, replacing γ^* by q^* in (5) will not significantly affect the estimate of H_P at $q^* \ll 1$.) Condensation rate S normalized by the integral in the denominator of (5) is the probability that a given hydrometeor reaching the surface has fallen from a height between z and $z + dz$. The last expression in (5) is obtained by integrating the first expression by parts and taking into account that the upward flux of air wN is approximately independent of z , that is, $\partial(Nw)/\partial z = 0$ (see Appendix for details).

We note that Eqs. (4) and (5) assume that γ decreases with height solely because of condensation that occurs in the rising air parcel; possible mixing with ambient air that can lead to a change in γ is neglected. In the real atmosphere the integration in (5) should be made over those height intervals where the mean ambient relative humidity is sufficiently high for condensation to occur, e.g., a threshold of $R_H(z) > 80\%$ can be applied (Lord and Franklin 1990). Under the assumption of constant Nw , the vertical profile of precipitation $P(z) = \int_z^{z_2} S(z')dz'$ coincides in form with the vertical profile of $\gamma^*(z)$ in the area of condensation: we should observe $P(z)/P_s = \gamma^*(z)/\gamma^*(z_1)$ at $z_1 \leq z \leq z_2$. Where the relative humidity is low but re-evaporation can be neglected, we should observe $P(z)/P_s$ stays approximately constant independent of changes in $\gamma(z)$.

3. Numerical estimates of H_P

The advantage of Eq. (5) is that H_P can be estimated from theory. Water vapor condenses as the moist saturated air ascends and cools. We allow for the incompleteness of condensation

which we can define as $\zeta \equiv \gamma^*(z_2)/\gamma^*(z_1)$, which describes the share of water vapor that has not condensed when the saturated air parcel rising from z_1 has reached z_2 . For a fully saturated atmosphere with surface relative humidity of $R_H = 100\%$ we have $z_1 = 0$, $z_2 = \infty$ in (5) and $\zeta = 0$. When the vertical distribution of water vapor follows the moist adiabat, H_P is unambiguously determined by the surface temperature (see Appendix). In Fig. 1A we show the dependence of moist adiabatic H_P on surface temperature T_s at a relative humidity of $R_H = 100\%$ and three values of ζ : 0, 1/2 and 2/3.

We can see that H_P grows with increasing surface temperature T_s , e.g. at $\zeta = 0$ we have $H_P = 3.5$ km at 290 K and 5.3 km at 300 K, i.e. H_P increases by around 50% for a 10 degrees rise in surface temperature. We also find that H_P decreases sharply with increasing ζ : at 300 K and $\zeta = 1/2$ we have $H_P = 2.4$ km, Fig. 1A, i.e. H_P decreases more than two-fold compared to the case of complete condensation $\zeta = 0$. Height z_2 at $\zeta = 1/2$ and $T_s = 300$ K is equal to 4.9 km, Fig. 1A.

In the real atmosphere the lower layer $z < z_1$ is generally undersaturated with a global mean relative humidity at the surface of about $R_H = 80\%$. Value of z_1 depends on the temperature lapse rate in the lower atmosphere $\Gamma_1 \equiv -\partial T/\partial z$ at $z < z_1$ (see Appendix). In Figs. 1B, 1C, and 1D values of z_1 and a moist adiabatic H_P at $\zeta = 0$ are given for R_H of 80, 60 and 40%, respectively, as dependent on surface temperature for three representative values of Γ_1 : 5, 6.5 and 9.8 K km⁻¹.

We find that the existence of the undersaturated layer $z < z_1$ does not significantly change H_P as compared to the case of $R_H = 100\%$. For example, at $T_s = 300$ K we have $z_1 = 0$ km and $H_P = 5.3$ km for $R_H = 100\%$, Fig. 1A, while for $R_H = 80\%$ we have $z_1 = 1.2$ km, $H_P = 5.6$ km at $\Gamma_1 = 5.0$ K km⁻¹ and $z_1 = 0.46$ km, $H_P = 5.0$ km at

$\Gamma_1 = 9.8 \text{ K km}^{-1}$, Fig. 1B. The value of z_1 grows with decreasing relative humidity. At $R_H = 40\%$, $T_s = 300 \text{ K}$ and $\Gamma_1 = 5 \text{ K km}^{-1}$ we have $z_1 = 4.4 \text{ km}$ and $H_P = 7.3 \text{ km}$, Fig. 1D. However, under conditions of low relative humidity, the temperature lapse rate cannot be much smaller than the dry adiabatic lapse rate, so the estimate of $H_P = 7.3 \text{ km}$ is not realistic. In the realistic case of $\Gamma_1 = 9.8 \text{ K km}^{-1}$ at $R_H = 40\%$ we have $z_1 = 1.8 \text{ km}$ and $H_P = 4.8 \text{ km}$. In other words, despite the condensation zone being elevated by z_1 when compared to the case of 100% relative humidity, the mean height of condensation H_P does not rise by the same magnitude. This is caused by the temperature dependence of H_P : at $z_1 \sim 1 \text{ km}$, temperature T_1 at z_1 is several degrees lower than at the surface, $T_1 < T_s$, such that the zone of intense condensation is compressed into a smaller vertical space than it would be at $T_1 = T_s$. So the resulting H_P can be even lower than in the case of $z_1 = 0$.

It is now possible to evaluate W_t from (2) at stated values of H_P and P_s to see if our assumption $W_t \gg |w|$ is realistic. Equating (2) and (3) we obtain $\overline{W}_t = P_s H_P / C$, where $C \equiv \int_0^\infty \rho_c dz$ is the amount of condensate and \overline{W}_t is the mean vertical velocity of condensate in the column. We take the mean precipitation in the tropical region between 30° S and 30° N to be $P_s = 1.3 \text{ m year}^{-1}$ according to the data of Legates and Willmott (1990), a conservative (i.e. low) value of $H_P = 3.8 \text{ km}$ (this corresponds to $T_s = 300 \text{ K}$, $R_H = 80\%$ and $\Gamma = 6.5 \text{ K km}^{-1}$ at $z > 0$, curve 7 in Fig. 1B) and $C \approx 10^{-1} \text{ kg m}^{-2}$ (Wood et al. 2002). Using these values we obtain $\overline{W}_t \approx 1.6 \text{ m s}^{-1}$. This value is about two orders of magnitude larger than typical time-averaged large-scale vertical air velocities $w < 1 \text{ cm s}^{-1}$ observed in the tropics (e.g., Rex 1958). We conclude that our assumption $W_t \gg |w|$ is reasonable.

We now consider the case of small terminal velocities, for which Eq. (3) does not hold. Terminal velocity depends on the size of hydrometeors and turns to zero when the condensate

particles become vanishingly small. The limiting case is the so-called “reversible adiabat”, which corresponds to $W_t = 0$ when all condensate travels together with the air and fully evaporates in the region where the moist air descends. Note that surface precipitation in this case is zero so Eq. (3) is inapplicable.

In order to travel with the air and to reach heights that are significantly larger than H_P , the condensate must have a vertical velocity comparable to that of air, $w_c \simeq w$ and $W_t \ll |w|$. For $C \sim 10^{-1} \text{ kg m}^{-2}$ and $W_t \ll |w| < 10^{-2} \text{ m s}^{-1}$ in the tropics we obtain from (2) $D < 10^{-2} \text{ W m}^{-2}$. In other words, even if all condensate in the tropical atmosphere consisted of the smallest condensate particles, their contribution to dissipation rate would not have exceeded 10^{-2} W m^{-2} . This means that in the tropics the small amount of condensed water that is brought by air updrafts to large altitudes significantly exceeding H_P (5) makes little contribution to dissipation rate D (3), (5), the latter being of the order of 1 W m^{-2} .

4. Condensation incompleteness and precipitation efficiency

As saturated moist air rises it can mix with drier air from the surroundings. This means that its γ (4) drops not because of condensation, but because of dilution through turbulent mixing: water vapor is replaced by dry air in the updraft. In such cases condensation is incomplete: the water vapor removed from the ascending air by turbulence has not condensed. This will affect the value of the so-called precipitation efficiency ε . In empirical studies this measure, ε , is defined as the ratio of precipitation P_s at the ground to the inflow of moisture

into the updraft. It is commonly observed to be in the vicinity of 20-40% (Fankhauser 1988).

A common interpretation of these low ε values from observation is that it reflects major re-evaporation of condensed water in downdrafts (Newton 1966; Foote and Fankhauser 1973). This presumes that all water vapor that has flown into the updraft will condense. Since condensation occurs when the relative humidity is equal to unity, this logic would imply that the relative humidity within the updraft should remain high up to the layer where the water vapor mixing ratio has dropped to a negligible value compared to its value at the surface. For example, for a moist adiabat at $T_s = 300$ K a hundredfold reduction corresponds to a height of about 14 km, Fig. 2A. In reality, however, relative humidity drops abruptly much earlier – for example, in hurricanes and their ambient environment it decreases sharply from over 80% to 50-60% at a height of about 4-5 km (Sheets 1969; Lord and Franklin 1990). The updraft of air carrying the smallest droplets high to the troposphere can continue beyond that height, but low relative humidity means that intense condensation cannot.

In other words, precipitation efficiencies $\varepsilon < 1$ do not necessarily imply re-evaporation of condensed moisture: rather, a low ratio of precipitation to the water vapor influx can indicate an incomplete condensation. Ignoring evaporation, from a simple mass balance consideration we have $(1 - \zeta)\rho_{vs}w_s = P_s$, where ρ_{vs} is the density of water vapor and w_s is the vertical air velocity at the cloud base, $\zeta \equiv \gamma^*(z_2)/\gamma^*(z_1) \simeq q^*(z_2)/q^*(z_1)$ is equal to the ratio of the water vapor mixing ratio at height z_2 where condensation discontinues and its value at the cloud base $z = z_1$. The flux of water vapor flowing into the cloud is given by $\rho_{vs}w_s$. In this case precipitation efficiency ε is equal to $\varepsilon = P_s/(\rho_{vs}w_s) = 1 - \zeta$. If $\varepsilon = 1/3$, this means $\zeta = 2/3$, i.e. the condensation zone reaches upward to a height where the water vapor mixing ratio decreases by one third as compared to its value at the cloud base. As we

show in Fig. 1A, high values of ζ and, hence, low precipitation efficiencies ε are associated with relatively low precipitation path length H_P .

5. Comparison with the results of Pauluis et al. (2000)

Pauluis et al. (2000) based their estimate of D , the first of this kind in the meteorological literature (Rennó 2001; Pauluis et al. 2001), on Eq. (3). They noted that, if re-evaporation is neglected, H_P is equal to the average height where condensation occurs. This is correct, but some of the subsequent assumptions and derivations are less well justified. Equation (5) of Pauluis et al. (2000) meant to define H_P as $H_P = \int_0^\infty q^* dz$, where q is water vapor mixing ratio, misses the normalization factor $q_s \equiv q(0)$ in the denominator (cf. our Eq. (5) above at $z_1 = 0$, $z_2 = \infty$ and $z_2 \gamma^*(z_2) = 0$). Turning to quantitative estimates, Pauluis et al. (2000) proposed that the scale height of the saturated water vapor mixing ratio in the tropics is about 2.5-3 km. Pauluis et al. (2000) do not offer any clear reasoning for this figure but refer to Emanuel and Bister (1996). Our reading of Emanuel and Bister (1996, p. 3284) finds only a mention of a certain “scale height for water vapor” of around 3 km. However, the scale height of saturated water vapor and the scale height of its mixing ratio are different atmospheric characteristics. They depend differently on temperature and, hence, height. In the tropical troposphere, for example, they range from 0 km to 5 km and to 10 km, for the scale height of water vapor and its mixing ratio, respectively (e.g., Makarieva et al. 2010, Fig. 1).

Leading on from their initial suggestions, Pauluis et al. (2000) offered several arguments as to why H_P in (3) should be several times higher than the scale height of the saturated

water vapor mixing ratio and takes a value of 5-10 km. First, they noted that the real precipitation path length H_P is greater than condensation height obtained from a moist adiabat because there is an undersaturated region in the subcloud layer. As we discussed in Section 3, while real, the effect is small and does not necessarily lead to an increase in H_P .

Second, Pauluis et al. (2000) proposed that an increase in H_P can be induced by the entrainment of the unsaturated air parcels into the region of saturated ascent. They did not, however, specify a mechanism for this. The entrainment of dry air causes the temperature lapse rate to rise above the moist adiabatic value, such that the temperature drops more rapidly with height. If, despite the dry air entrainment, the condensation nevertheless continues in the updraft prompted by this additional cooling in the ambient environment, the change in local lapse rate will reduce rather than raise the mean condensation height H_P . Curve 7 in Fig. 1B illustrates the dependence of H_P on T_s for $R_H = 80\%$ and a mean tropospheric lapse rate of 6.5 K km^{-1} instead of moist adiabatic lapse rate. In this case H_P depends little on surface temperature and ranges between 3 and 4 km. If, on the other hand, condensation is discontinued by the drop in relative humidity associated with the removal of water vapor and its replacement by dry air in the region of ascent, then H_P is limited by the height where the dry air entrainment occurred. In neither case does H_P increase.

Pauluis et al. (2000) also mention that the real precipitation path length is increased by the fact that some hydrometeors are lifted by updrafts to high altitudes. However, as discussed Section 2, such hydrometeors are small and possess terminal velocities that are much smaller than air velocity, such that Eq. (3), which Pauluis et al. (2000) intended to use, is thus inapplicable. On average, these hydrometeors make only a negligible contribution to the total dissipation rate associated with precipitation owing to both their slow terminal

velocity and their small combined mass.

The final argument put forward by Pauluis et al. (2000), and the only quantitative one, concerns re-evaporation. They presume that this effect can lead to a significant underestimate of the real value of H_P . Pauluis et al. (2000) quote the work of Fankhauser (1988) and Ferrier et al. (1996) to support the statement that a significant part (from half to two-thirds) of all condensed moisture actually re-evaporates and does not hit the ground. From this Pauluis et al. (2000) suggest that if evaporation occurs uniformly as the hydrometeors are falling, this process increases the effective precipitation path length by a factor of 1.5-2. We note for the record that Fankhauser (1988), who investigated empirical data on the water budget of convective clouds including precipitation efficiency, does not mention any quantitative estimate of the re-evaporation of condensed moisture. Ferrier et al. (1996, p. 2105), on the other hand, do report the magnitude of re-evaporation as compared to total condensation within a squall, but their results come from a numerical model rather than observational evidence. In order to estimate the actual rate of evaporation of condensate in the downdrafts we would need to perform careful estimates of condensate transport within the cloud – rather than measuring the transport of total moisture that is dominated by water vapor. Estimates of sufficient accuracy are not available. We can, in contrast, be confident that the effect of incomplete condensation associated with low precipitation efficiency is real. But, as discussed in the previous section, this will decrease rather than increase the estimate of H_P .

Furthermore, even if evaporation in downdrafts did constitute a significant fraction of total condensation, the suggestion of Pauluis et al. (2000) about a 1.5-2 increase in effective H_P would still be incorrect. Let us first see how this conclusion was reached, because

Pauluis et al. (2000) do not explain this in any detail. The argument of Pauluis et al. (2000) derives from Eq. (3) along with the one-dimensional continuity equation for condensate particles. If $j_P \equiv \rho_c(z)W_t$ is the downward flux of condensate at point z , then the continuity equation is $\partial j_P/\partial z = E$, where $E > 0$ is evaporation. If, following Pauluis et al. (2000), we assume that E is constant and that $j_P(0) = (1/3)j_P(H_P)$ (evaporation has decreased the original precipitation flux by two thirds as it traveled from $z = H_P$ to $z = 0$), then we have $j_P(z) = j_P(0)(1 + 2z/H_P)$. This allows us to calculate D from (2) as $D = \int_0^{H_P} j_P g dz = 2j_P(0)gH_P = 2P_s g H_P$. Had this logic been correct, we could conclude, as did Pauluis et al. (2000), that Eq. (3) indeed underestimates the real dissipation by half.

There are, however, two errors in this reasoning. The first one consists in neglecting the fact that local dissipation rate $\rho_c g W_t$ and local evaporation with respect to droplet size behave differently. Since absolute evaporation rate is proportional to droplet area, the smallest droplets evaporate most rapidly. If we have equal amounts M (g) of small droplets with radius r_1 and large droplets with radius $r_2 > r_1$, the rate of depletion of total condensate from the evaporation of small droplets will be r_2/r_1 times faster than from large droplets (evaporation rate $\propto Ns \propto (M/m)r^2 \propto M/r$, where $s \propto r^2$ is droplet's surface area, $N \propto M/m \propto M/r^3$ is the number of droplets, $m \propto r^3$ is droplet mass). In comparison, because of the fact that terminal velocity grows with increasing droplet radius, the contribution of the small droplets to total dissipation will be lower than that of the large droplets. In theory, for spherical droplets with $W_t \propto r^2$, it will be lower by $(r_2/r_1)^2$ times. For example, with $r_2/r_1 = 10$, 90% of all evaporation will come from droplets that make a 1% contribution to total dissipation.

The second error in their reasoning is that they implicitly use $j_P \equiv \rho_c(z)W_t$ to rep-

resent the downward flux of condensate. This neglects the important role of vertical air movements in transporting the smallest condensate particles. Rather they should have used $j_c = \rho_c(z)(w - W_t)$, where $w < 0$ is the downward velocity of air. The w term is particularly important in consideration of evaporation, because the smallest droplets with $W_t \ll -w$ are so slow that they can be only transported by the downdraft. This means that the continuity equation $\partial j_P / \partial z = E$ underlying the reasoning of Pauluis et al. (2000) is not valid. The correct equation $\partial j_c / \partial z = E$ does not offer any insights regarding the frictional dissipation of D in the column because the distribution of w remains unknown.

To summarize, we find no support for the claim of Pauluis et al. (2000) that precipitation path length should be several times higher than the value of H_P given by (5).

6. Numerical estimate of D

We have shown that H_P grows with increasing incompleteness of condensation ζ , increasing surface temperature and decreasing lapse rate Γ_1 at $z < z_1$, Fig. 1. Among these, the incompleteness of condensation ζ is both the least known and the most influential, Fig. 1A. It is closely linked to convection depth. We suggest that the uncertainty of the mean D values for the tropical region is largely determined by the uncertainty in H_P , which is, in its turn, largely reflects uncertainty of ζ . Taking $T_s = 300$ K as the mean surface temperature during precipitation in the tropical region, $\Gamma_1 = 5$ K km⁻¹ and $R_H = 80\%$, we obtain $H_P = 5.6$ km for complete condensation $\zeta = 0$, Fig. 1B. At the lower end is the estimate of H_P obtained assuming $\zeta = 2/3$ (corresponding to a low precipitation efficiency of $\varepsilon = 1/3$), which at $T_s = 300$ K, $\Gamma_1 = 5$ K km⁻¹ and $R_H = 80\%$ gives $H_P = 2.5$ km.

Pauluis et al. (2000) estimated D from the mean latent heat flux Q instead of precipitation $P = Q/L_v$ in the tropics considering that $D/Q = gH_P/L_v$, where $L_v = 2.5 \times 10^6 \text{ J kg}^{-1}$ is the heat of vaporization. Using $Q = 100 \text{ W m}^{-2}$ and H_P values of 2.5 and 5.6 km we obtain a range of 1.0-2.2 W m^{-2} for the mean tropical value of D .

For the global mean temperature $T_s = 288 \text{ K}$ at $R_H = 80\%$ and $\Gamma_1 = 6.5 \text{ K km}^{-1}$ we have $H_P = 3.6 \text{ km}$ for $\zeta = 0$, Fig. 1B, and $H_P = 1.5 \text{ km}$ for $\zeta = 2/3$. Using the mean value of 2.5 km and mean global precipitation of 1 m year^{-1} (L'vovitch 1979) we obtain a global mean value of $D \sim 0.78 \text{ W m}^{-2}$ from (3). This means $4 \times 10^{14} \text{ W}$ for Earth as a whole and $1.2 \times 10^{14} \text{ W}$ for the gravitational power of precipitation on land. (We note that the estimate of 10^{14} W for land was previously obtained based on Eq. (3) in a different context discussing renewable energy sources (Gorshkov 1982, p. 6).)

If the vertical profile of precipitation $P(z)$ is known, the value of D can be estimated directly from (2) under the assumption that $P(z) = \rho_c(z)W_t$. This was recently done by Pauluis and Dias (2012) who used satellite-derived $P(z)$ profiles from the Tropical Rainfall Measurement Mission and estimated D for the tropical region between 30° S and 30° N to be 1.8 W m^{-2} . Using this value Pauluis and Dias (2012) went on to estimate H_P from Eq. (3) by dividing D (2) by $P_s g$, $H_P = D/(P_s g)$. Having obtained values of 5.1 km for the ocean and 6.9 km for land, Pauluis and Dias (2012) concluded that these results agree with their earlier estimates of 5-10 km for H_P in the tropics (Pauluis et al. 2000). They proposed that the larger value obtained over land indicates more intense convection than over the ocean.

The derivation of precipitation rates from the satellite radar data involves considerable uncertainties. The estimation process involves a large number of empirical relationships between reflectivity and precipitation rates as well as various assumptions concerning the prop-

erties of the hydrometeors like their size distribution and terminal velocity (e.g., Uijlenhoet 2001; Durden et al. 1998; Bowman 2005; Prat and Barros 2009). The commonly used algorithms perform differently over land than they do over oceans (Prat and Barros 2009). They also perform differently on the ground surface versus at the top of clouds (Durden et al. 1998). The estimate of 1.8 W m^{-2} reported without any quantified assessment of the associated uncertainties ranges does not constrain D any more accurately than do theoretical estimates, although it can be noted that this estimate falls out of the $2\text{-}4 \text{ W m}^{-2}$ established for the tropical region by Pauluis et al. (2000).

Moreover, our examination of the precipitation profiles $P(z)$ shown in Fig. 2 of Pauluis and Dias (2012) raises further problems. These data support neither the estimate of $D = 1.8 \text{ W m}^{-2}$ reported for the tropical region as a whole, nor the estimates of H_P made for land and ocean. Indeed, integrating these profiles yields a value of 1.4 W m^{-2} for all the three profiles (the tropics as a whole, land and ocean). This 30% discrepancy raises further questions concerning the validity of the numerical estimates reported by Pauluis and Dias (2012). The discrepancy illustrates the potential inaccuracy associated with using satellite radar data on precipitation. Heights H_P estimated from the corrected values of D using $P_s = 2.6 \text{ mm day}^{-1}$ for ocean and $P_s = 2.1 \text{ mm day}^{-1}$ for land yields $H_P = 4.7 \text{ km}$ for the ocean and $H_P = 5.7 \text{ km}$ for land instead of, respectively, 5.1 km and 6.9 km obtained by Pauluis and Dias (2012).

Furthermore, the derivation of H_P from Eq. (3) is potentially misleading, as such an estimate is sensitive to the estimate of surface precipitation. Satellite radar based assessments of precipitation are based on the reflectivity coefficient of precipitating particles. The radar is unable to accurately distinguish surface precipitation because of the high reflectivity of the surface. Note for example, that if surface precipitation is underestimated in the lowest

kilometer, this may make little impact on the column-integrated D (2), but will have a considerable impact on the value of H_P . (We also note that precipitation rates in the upper part of the atmosphere can be, on the contrary, overestimated by the radar (Durden et al. 1998).) According to Fig. 2 of Pauluis and Dias (2012), precipitation in the lowest 1 km makes about a 1/5 contribution to the column-integrated value of D . If surface precipitation in this lowest region is underestimated by 25% (Durden et al. 1998; Bowman 2005) and constitutes 75% of the real value, this corresponds to a $25\%/5 = 5\%$ underestimate in total D . But $H_P = D/(gP_s)$ is then overestimated by a factor of $(100-5)\%/75\% = 1.3$. Applying this additional correction factor to our corrected H_P estimates we obtain $H_P = 4.7/1.3 = 3.6$ km instead of 5.1 km for the ocean and $H_P = 5.7/1.3 = 4.4$ km instead of 6.9 km for land. Both values are outside the 5-10 km range of Pauluis et al. (2000), but within the 3-5 km range estimated from our theoretical analysis. We also note that these values are close to $H_P = 3.8$ km that at 80% surface relative humidity is characteristic of the mean tropospheric lapse rate 6.5 K km^{-1} in a saturated atmosphere at $T_s = 300 \text{ K}$, see curve 7 in Fig. 1B.

Tropical land include some exceptionally wet regions like the Amazon and Congo forests, where precipitation is 2-3 times higher than over the nearby ocean (Makarieva et al. 2012). But the tropics also include very dry regions such as the Sahara desert and the Australian interior. Combining these wet and dry regions under one and the same category and calculating a single mean precipitation profile for all tropical *land*, as done in Fig. 2 of Pauluis and Dias (2012), is of questionable value given the diversity of physical settings. (Note that these concerns have less significance for a tropic-wide estimate the values of which are dominated by the oceans). In the driest regions of the Earth where surface precipitation tends to zero, estimating H_P from surface precipitation lacks any physical meaning, as $H_P \rightarrow \infty$

at $P_s \rightarrow 0$. Thus any estimated value for H_P does not carry any information about the real vertical distribution or intensity of precipitation. We note in this context that while Pauluis and Dias (2012) concluded that high values of H_P over land are indicative of a more intense convection, judging from their Fig. 3 one might also think that the region of most intense convection on Earth is the inner part of Sahara desert. Here H_P , as estimated with use of the near zero value of surface precipitation, reaches beyond 10 km (Pauluis and Dias 2012, Fig. 3). This apparently nonsensical result illustrates the need to have a consistent theoretical basis for any analysis of empirical evidence.

As we discussed in Section 2, in a saturated atmosphere the vertical profile of precipitation $P(z)/P_s$ should coincide with the vertical profile of $\gamma^*(z)/\gamma(0)$. In Figs. 2B, 2C, and 2D the mean vertical profile of tropical precipitation taken from Fig. 2 of Pauluis and Dias (2012) is contrasted against theoretical profiles of $\gamma^*(z)/\gamma(0)$ calculated for different values of surface temperature, relative humidity and temperature lapse rate. We see that saturated moist adiabatic profiles of $\gamma^*(z)/\gamma(0)$ tend to overestimate $P(z)/P_s$ in the upper atmosphere, Figs. 2B and 2C. The observed mean profile $P(z)/P_s$ is confined between $\gamma^*(z)/\gamma(0)$ profiles built for surface relative humidity from 80% to 40% and having a constant lapse rate of $\Gamma = 6.5 \text{ K km}^{-1}$, Fig. 2D.

7. Discussion

In order to investigate how an atmospheric phenomenon responds to changes in atmospheric parameters it is important to establish a sound theoretical basis concerning the key physical relationships. In this paper, building from basic physical principles and relation-

ships, we evaluated the rate of turbulent frictional dissipation associated with precipitation. We discussed how precipitation path length, H_P , is the key parameter controlling this rate, and investigated how it depends on surface temperature, humidity and the vertical extent of the area where condensation occurs.

We now consider how the frictional dissipation relates to the dynamic power of atmospheric circulation. We can illustrate this relationship with a simple example. Consider a hanging weight tied with a short rope to an extended spring. The system is in a state of equilibrium with the weight exactly balanced by the tension of the spring. When we cut the rope the weight can fall. At this moment two types of potential energy have become available: the first is the weight's energy in the gravitational field and the second is the energy of the stretched spring. The first potential energy is transformed to kinetic energy as the weight falls, while the second potential energy is transformed to kinetic energy as the spring accelerates upward. It is clear from this example that the two potential energies are independent in magnitude: the first depends on the initial height of the weight above the surface, the second depends on the elasticity of the spring and is independent of height and of what happens to the weight after the rope is cut.

Likewise upon condensation, two types of potential energy are formed: first the potential energy of falling hydrometeors as dictated by the precipitation path length H_P (5) and second the potential energy of the non-equilibrium pressure gradient that results from the disappearance of water vapor from the gas phase. The key peculiarity of this second process consists in the fact that this potential energy is coupled to the vertical motion of moist air and is released only when the air moves upwards.

Since precipitation and condensation always accompany each other, it is of interest to

compare the powers associated with each of the two processes and how these might influence atmospheric motion. Previously we have argued that the dynamic power of condensation-induced circulation D_c (W m^{-2}) per unit surface area can be estimated as $D_c = P_s RT/M_v$, where $R = 8.3 \text{ J mol}^{-1} \text{ K}^{-1}$ is the universal gas constant and T is the mean temperature in the atmospheric column where condensation occurs (Makarieva et al. 2010; Makarieva and Gorshkov 2011; Gorshkov et al. 2012). This formula results from the proposition that the dynamic power \mathcal{D}_c (W m^{-3}) per unit air volume of the upward pressure gradient force induced by condensation and associated with the non-equilibrium vertical gradient of saturated water vapor, is equal to

$$\mathcal{D}_c = w \left(\frac{\partial p_v^*}{\partial z} - \gamma \frac{\partial p}{\partial z} \right) = wp \frac{\partial \gamma^*}{\partial z} = RT S, \quad (6)$$

where $S = wN\partial\gamma^*/\partial z$ is the net condensation rate per unit volume in $\text{mol H}_2\text{O m}^{-3} \text{ s}^{-1}$, N (mol m^{-3}) is molar density of air, see (4). Neglecting the minor dependence of $T \simeq T_s$ on z and observing that the integral of S over z is equal to P_s/M_v , see Appendix, we have

$$D_c = \int_0^\infty \mathcal{D}_c dz = \frac{P_s RT_s}{M_v}. \quad (7)$$

To illustrate the value of this theoretical result we can now estimate the global power of condensation-induced circulation. Using a global mean value of P_s of 1 m year^{-1} (L’vovitch 1979; Legates and Willmott 1990) and global mean surface temperature of $T_s = 288 \text{ K}$, we have $D_c = 4 \text{ W m}^{-2}$. For the tropical region with mean $P_s = 1.3 \text{ m year}^{-1}$ we have $D_c = 5.5 \text{ W m}^{-2}$. Since under conditions of hydrostatic equilibrium the work done by the vertical pressure gradient is compensated by the work done by gravity, the kinetic energy of the large-scale air flow derives from the horizontal pressure gradient alone. The power of this horizontal force per unit air volume is equal to $u\partial p/\partial x$, where u is the horizontal velocity

component parallel to the horizontal pressure gradient. The dynamic power of atmospheric circulation (the rate at which the kinetic energy is generated) can therefore be estimated from the observed horizontal pressure gradients and the observed u values. It can also be estimated as the power of turbulent dissipation of the air flow under the assumption that in the stationary case the dynamic power that creates the kinetic energy is equal to the power of turbulent dissipation D_t of this energy. The available global mean observation-based estimates of these powers are in the range of 2-4 W m⁻² (Oort 1964; Lorenz 1967; Peixoto and Oort 1992). Our global mean estimate, derived from basic principles, falls at the upper edge of this range.

The ratio of the powers of the two processes - the frictional dissipation power D of hydrometeors and the dynamic power D_c of condensation-induced circulation - is given by

$$\frac{D}{D_c} = \frac{H_P}{h_v}, \quad h_v \equiv \frac{RT_s}{M_v g}. \quad (8)$$

This ratio does not depend on precipitation rate P_s but grows with temperature owing to the dependence of H_P on T_s , Fig. 1. The value of h_v (8) has the meaning of the scale height of (unsaturated) water vapor in hydrostatic equilibrium, at $T_s = 300$ K it is equal to 14 km. With the large-scale values of H_P not exceeding 6 km at mean surface temperatures not exceeding 300 K, Fig. 1, we obtain a general estimate of $D/D_c < 0.4$.

Noting that D grows with surface temperature, Fig. 1, we can estimate when D exceeds D_c . We do this using (8) and assuming that the budget of energy turnover for a condensation-induced circulation has the form of $D_c = D_t + D$, where D_t is turbulent dissipation of the large-scale air flow. At $R_H = 80\%$ and $\Gamma_1 = 5$ K km⁻¹ D equals D_c at $T_s = 323$ K, Fig. 1B. At higher temperatures in a moist adiabatic atmosphere any significant circulation due to

condensation will be prevented because of the insufficient dynamic power to overcome the energy losses associated with frictional dissipation due to precipitation. If the atmosphere is not moist adiabatic but has a constant lapse rate of $\Gamma = 6.5 \text{ K km}^{-1}$, D grows much more slowly with increasing surface temperature (see Fig. 1, curves 7). It does not approach D_c anywhere at $T_s < 360 \text{ K}$, i.e. in the entire range where the approximation $\gamma \ll 1$ on which Eq. (5) is based holds. From these considerations we conclude that frictional dissipation due to precipitation is insufficient to arrest condensation-induced atmospheric circulation on Earth.

APPENDIX

Equations for calculating z_1 and H_P

Eq. (5) is obtained using (4) and considering that

$$\begin{aligned} \int_{z_1}^{z_2} S(z)zdz &= wN\gamma^*z \Big|_{z_2}^{z_1} + \int_{z_1}^{z_2} wN\gamma^*dz + \int_{z_1}^{z_2} \frac{\partial(wN)}{\partial z}\gamma^*zdz \\ &\simeq wN \left\{ \gamma^*z \Big|_{z_2}^{z_1} + \int_{z_1}^{z_2} \gamma^*dz \right\}, \end{aligned} \quad (\text{A1})$$

$$\begin{aligned} \int_{z_1}^{z_2} S(z)dz &= wN\gamma^* \Big|_{z_2}^{z_1} + \int_{z_1}^{z_2} \frac{\partial(wN)}{\partial z}\gamma^*dz \\ &\simeq wN\gamma^* \Big|_{z_2}^{z_1}. \end{aligned} \quad (\text{A2})$$

From the one-dimensional stationary continuity equation we have $\partial(wN)/\partial z = -S$. This means that the terms discarded in (A1) and (A2) constitute a small magnitude of the order of $\gamma^* \ll 1$ as compared to the initial terms. Quantity wN changes little with z (by a relative magnitude of the order of γ^*) as compared to γ^* that changes severalfold. Therefore Nw can be assumed to be constant and cancelled from both the denominator and nominator in ratio (5). The inaccuracy of the resulting expression for H_P (5) is of the order of γ^* and, for temperatures of interest, does not exceed 10%.

The system of equations for moist adiabat solved to calculate H_P in Fig. 1A is as follows

(Makarieva et al. 2010; Gorshkov et al. 2012):

$$\frac{1}{T} \frac{\partial T}{\partial z} - \frac{\mu}{p} \frac{\partial p}{\partial z} + \frac{\mu \xi}{1 - \gamma^*} \frac{\partial \gamma^*}{\partial z} = 0, \quad (\text{A3})$$

$$\frac{1}{\gamma^*} \frac{\partial \gamma^*}{\partial z} - \frac{\xi}{T} \frac{\partial T}{\partial z} + \frac{1}{p} \frac{\partial p}{\partial z} = 0, \quad (\text{A4})$$

$$-\frac{1}{p} \frac{\partial p}{\partial z} - \frac{Mg}{RT} = 0, \quad (\text{A5})$$

where temperature T , air pressure p , and $\gamma^* \equiv p_v^*/p$ – the relative partial pressure of saturated water vapor – are functions of height z . Here $\xi \equiv L_v/(RT)$, $L_v = 45 \times 10^3 \text{ J mol}^{-1}$ is heat of vaporization, $R = 8.3 \text{ J mol}^{-1} \text{ K}^{-1}$ is the universal gas constant, $M = (1 - \gamma^*)M_d + \gamma^*M_v$, $M_d = 29 \text{ g mol}^{-1}$, $M_v = 18 \text{ g mol}^{-1}$, $\mu = R/c_p = 2/7$, c_p is the molar heat capacity of air at constant pressure ($\text{J mol}^{-1} \text{ K}^{-1}$). Equation (A3) results from the first law of thermodynamics for moist air saturated with water vapor. Equation (A4) derives from the definition of γ^* combined with the Clausius-Clapeyron law. Equation (A5) is equivalent to the condition of hydrostatic equilibrium (1) for ideal gas.

The boundary conditions for the surface $z = 0$ at a given surface temperature T_s read

$$T = T_s, \quad (\text{A6})$$

$$p = p_s, \quad (\text{A7})$$

$$p_v^*(T) = p_{v0}^* \exp(\xi_0 - \xi), \quad (\text{A8})$$

where p_{v0}^* and $\xi_0 = L_v/(RT_0)$ correspond to some reference temperature T_0 . We take $T_0 = 303 \text{ K}$, $p_{v0}^* = 42 \text{ hPa}$ and the standard value for the atmospheric pressure $p_s = 1013 \text{ hPa}$. The dependence of vaporization heat L_v on temperature is neglected. In this case $\xi_0 = 18$.

For a fully saturated atmosphere $z_1 = 0$ in (5). Numerical evaluation of the system of Eqs. (A3)-(A5) allows us to obtain the unknown functions $T(z)$, $p(z)$, $\gamma^*(z)$ and to calculate

H_P (5) as shown in Fig. 1A.

In Figs. 1B, 1C, and 1D the atmosphere at the surface $z = 0$ is not saturated and has a relative humidity of 80%, 60% and 40%, respectively. To find height z_1 where the relative humidity reaches unity, we assume that within the range $0 \leq z \leq z_1$ the non-saturated $\gamma = p_v/p$ is constant and temperature $T(z)$ drops versus height z at a constant lapse rate Γ_1 , $T(z) = T_s - \Gamma_1 z$. Then the non-saturated pressure p_v of water vapor is given by

$$p_v(z) = p_v^*(T_s) R_H \frac{p(z)}{p_s}, \quad (\text{A9})$$

where R_H is relative humidity at the surface $z = 0$, saturated pressure p_v^* of water vapor is governed by the Clausius-Clapeyron law (A8) and pressure $p(z)$ conforms to the condition of hydrostatic equilibrium (A5) with $M \simeq M_d$. Height z_1 where relative humidity becomes unity and condensation commences, is a function of the surface temperature T_s . We find height z_1 as the solution of equation

$$p_v(z_1) = p_v^*(T_1), \quad T_1 \equiv T_s - \Gamma_1 z_1. \quad (\text{A10})$$

The atmosphere is assumed to be saturated and moist adiabatic within the range $z_1 \leq z \leq z_2$. We need to evaluate the system of Eqs. (A3)-(A5) in order to find functions $T(z)$, $p(z)$, and $\gamma^*(z)$. However, the boundary conditions should now be imposed not at the ground surface but at $z = z_1$, so that $T = T_1$ and $p = p(z_1)$ instead of T_s (A6) and p_s (A7) at $z = 0$. Using the obtained solutions, condensation rate is calculated from (5).

Curves 7 in Figs. 1B, 1C, and 1D are obtained for an atmosphere that is unsaturated at $z < z_1$, saturated at $z \geq z_1$ and has a constant temperature lapse rate of $\Gamma = 6.5 \text{ K km}^{-1}$ at $z \geq 0$. The solution at $z \geq z_1$ is obtained by solving the system of Eqs. (A4), (A5) and $\partial T/\partial z = -\Gamma$ instead of (A3).

REFERENCES

- Bowman, K. P., 2005: Comparison of trmm precipitation retrievals with rain gauge data from ocean buoys. *J. Clim.*, **18**, 178–190.
- Cotton, W. R., G. Bryan, and S. C. van den Heever, 2011: Fundamental equations governing cloud processes. *Int. Geophys.*, **99**, 15–52.
- Durden, S. L., Z. S. Haddad, A. Kitiyakara, and F. K. Li, 1998: Effects of nonuniform beam filling on rainfall retrieval for the trmm precipitation radar. *J. Atmos. Oceanic Technol.*, **15**, 635–646.
- Emanuel, K. A. and M. Bister, 1996: Moist convective velocity and buoyancy scales. *J. Atmos. Sci.*, **53**, 3276–3285.
- Fankhauser, J. C., 1988: Estimates of thunderstorm precipitation efficiency from field measurements in ccope. *Mon. Wea. Rev.*, **116**, 663–684.
- Ferrier, B. S., J. Simpson, and W.-K. Tao, 1996: Factors responsible for precipitation efficiencies in midlatitude and tropical squall simulations. *Mon. Wea. Rev.*, **124**, 2100–2125.
- Foote, G. B. and J. C. Fankhauser, 1973: Airflow and moisture budget beneath a northeast colorado hailstorm. *J. Appl. Meteor.*, **12**, 1330–1353.
- Gorshkov, V. G., 1982: *Energetics of the biosphere*. Leningrad Politechnical Institute, 80 pp.

- Gorshkov, V. G., A. M. Makarieva, and A. V. Nefiodov, 2012: Condensation of water vapor in the gravitational field. *J. Exp. Theor. Phys.*, **142**, in press, <http://arxiv.org/abs/1208.2581>.
- Jiang, H., J. B. Halverson, J. Simpson, and E. J. Zipser, 2008: On the differences in storm rainfall from hurricanes isidore and lili. part ii: Water budget. *Wea. Forecasting*, **23**, 44–61.
- Legates, D. R. and C. J. Willmott, 1990: Mean seasonal and spatial variability in gauge-corrected, global precipitation. *Int. J. Climatol.*, **10**, 111–127.
- Lord, S. J. and J. L. Franklin, 1990: The environment of hurricane debby (1982). part ii: Thermodynamic fields. *Mon. Wea. Rev.*, **118**, 1444–1459.
- Lorenz, E. N., 1967: *The nature and theory of the general circulation of the atmosphere*. World Meteorological Organization, 161 pp.
- L’vovitch, M. I., 1979: *World water resources and their future*. American Geophysical Union, 415 pp.
- Makarieva, A. M. and V. G. Gorshkov, 2007: Biotic pump of atmospheric moisture as driver of the hydrological cycle on land. *Hydrol. Earth Syst. Sci.*, **11**, 1013–1033.
- Makarieva, A. M. and V. G. Gorshkov, 2011: Radial profiles of velocity and pressure for condensation-induced hurricanes. *Phys. Lett. A*, **375**, 1053–1058.
- Makarieva, A. M., V. G. Gorshkov, and B.-L. Li, 2012: Revisiting forest impact on atmospheric water vapor transport and precipitation. *Theor. Appl. Climatol.*, **in press**, doi: 10.1007/s00704-012-0643-9.

- Makarieva, A. M., V. G. Gorshkov, D. Sheil, A. D. Nobre, and B.-L. Li, 2010: Where do winds come from? a new theory on how water vapor condensation influences atmospheric pressure and dynamics. *Atmos. Chem. Phys. Discuss.*, **10**, 24 015–24 052.
- Newton, C. W., 1966: Circulations in large sheared cumulonimbus. *Tellus*, **18**, 699–713.
- Oort, A. H., 1964: On estimates of the atmospheric energy cycle. *Mon. Wea. Rev.*, **92**, 483–493.
- Pauluis, O., V. Balaji, and I. M. Held, 2000: Frictional dissipation in a precipitating atmosphere. *J. Atmos. Sci.*, **57**, 989–994.
- Pauluis, O., V. Balaji, and I. M. Held, 2001: Reply. *J. Atmos. Sci.*, **58**, 1178–1179.
- Pauluis, O. and J. Dias, 2012: Satellite estimates of precipitation-induced dissipation in the atmosphere. *Science*, **335**, 953–956.
- Peixoto, J. P. and A. H. Oort, 1992: *Physics of Climate*. American Institute of Physics, 520 pp.
- Prat, O. P. and A. P. Barros, 2009: Exploring the transient behavior of z-r relationships: Implications for radar rainfall estimation. *J. Appl. Meteor. Climatol.*, **48**, 2127–2143.
- Rennó, N. O., 2001: Comments on “frictional dissipation in a precipitating atmosphere”. *J. Atmos. Sci.*, **58**, 1173–1177.
- Rex, D. F., 1958: Vertical atmospheric motions in the equatorial central pacific. *Geophysica*, **6**, 479–501.
- Schiermeier, Q., 2010: The real holes in climate science. *Nature*, **463**, 284–287.

Schneider, T., 2006: The general circulation of the atmosphere. *Annu. Rev. Earth Planet. Sci.*, **34**, 655–688.

Sheets, R. C., 1969: Some mean hurricane soundings. *J. Appl. Meteor.*, **8**, 134–146.

Uijlenhoet, R., 2001: Raindrop size distributions and radar reflectivity-rain rate relationships for radar hydrology. *Hydrol. Earth Syst. Sci.*, **5**, 615–627.

Wood, R., C. S. Bretherton, and D. L. Hartmann, 2002: Diurnal cycle of liquid water path over the subtropical and tropical oceans. *Geophys. Res. Lett.*, **29**, 2092.

List of Figures

- 1 Precipitation path length H_P as a function of surface temperature T_s at various values of surface relative humidity R_H : 100% (A), 80% (B), 60% (C), 40% (D).

A: Moist adiabat in a fully saturated atmosphere, $z_1 = 0$. Height of condensation area z_2 is equal to the height where $\zeta \equiv \gamma^*(z_2)/\gamma^*(z_1) = 0$ (triangles), $\zeta = 1/2$ (circles) or $\zeta = 2/3$ (squares).

B, C, D: Curves 1 – 3 denote z_1 , curves 4 – 7 denote H_P at $\zeta = 0$. Temperature lapse rate Γ_1 at $z < z_1$ is equal to 9.8 K km^{-1} (red squares), 6.5 K km^{-1} (blue circles, stars), 5 K km^{-1} (green triangles). At $z \geq z_1$ the atmosphere is moist adiabatic, except for curves 7, which are for an atmosphere that is saturated above z_1 and has a constant temperature lapse rate $\Gamma = 6.5 \text{ K km}^{-1}$ everywhere at $z \geq 0$ (see Appendix for details).

33

- 2 Vertical distribution of $\gamma^*(z)/\gamma(0)$ under different atmospheric conditions. Dashed curve denotes the mean observed tropical precipitation $P(z)/P(0)$ from Fig. 2 of Pauluis and Dias (2012).
- A: Moist adiabat in a completely saturated atmosphere, $R_H = 100\%$, cf. Fig. 1A.
- B: The atmosphere is unsaturated at $z < z_1$ ($R_H = 80\%$, $\Gamma_1 = 5 \text{ K km}^{-1}$) and moist adiabatic at $z \geq z_1$, cf. Fig. 1B.
- C: The atmosphere is unsaturated at $z < z_1$ and moist adiabatic at $z \geq z_1$.
- D: The atmosphere is unsaturated at $z < z_1$, saturated at $z \geq z_1$ and has a constant temperature lapse rate $\Gamma = 6.5 \text{ K km}^{-1}$ at $z \geq 0$ (cf. curves 7 in Figs. 1B, 1C, and 1D).

34

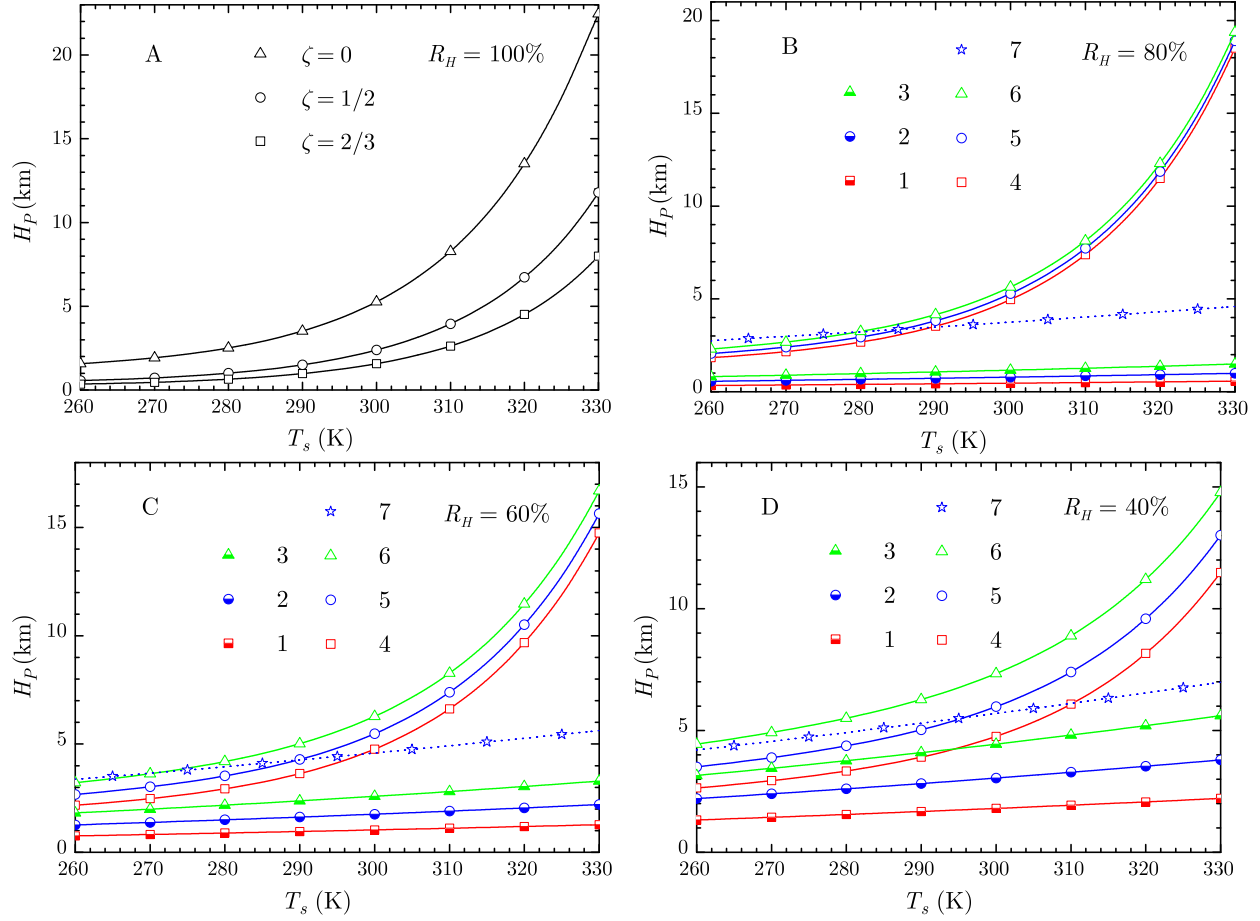


FIG. 1. Precipitation path length H_P as a function of surface temperature T_s at various values of surface relative humidity R_H : 100% (A), 80% (B), 60% (C), 40% (D).

A: Moist adiabat in a fully saturated atmosphere, $z_1 = 0$. Height of condensation area z_2 is equal to the height where $\zeta \equiv \gamma^*(z_2)/\gamma^*(z_1) = 0$ (triangles), $\zeta = 1/2$ (circles) or $\zeta = 2/3$ (squares).

B, C, D: Curves 1 – 3 denote z_1 , curves 4 – 7 denote H_P at $\zeta = 0$. Temperature lapse rate Γ_1 at $z < z_1$ is equal to 9.8 K km^{-1} (red squares), 6.5 K km^{-1} (blue circles, stars), 5 K km^{-1} (green triangles). At $z \geq z_1$ the atmosphere is moist adiabatic, except for curves 7, which are for an atmosphere that is saturated above z_1 and has a constant temperature lapse rate $\Gamma = 6.5 \text{ K km}^{-1}$ everywhere at $z \geq 0$ (see Appendix for details).

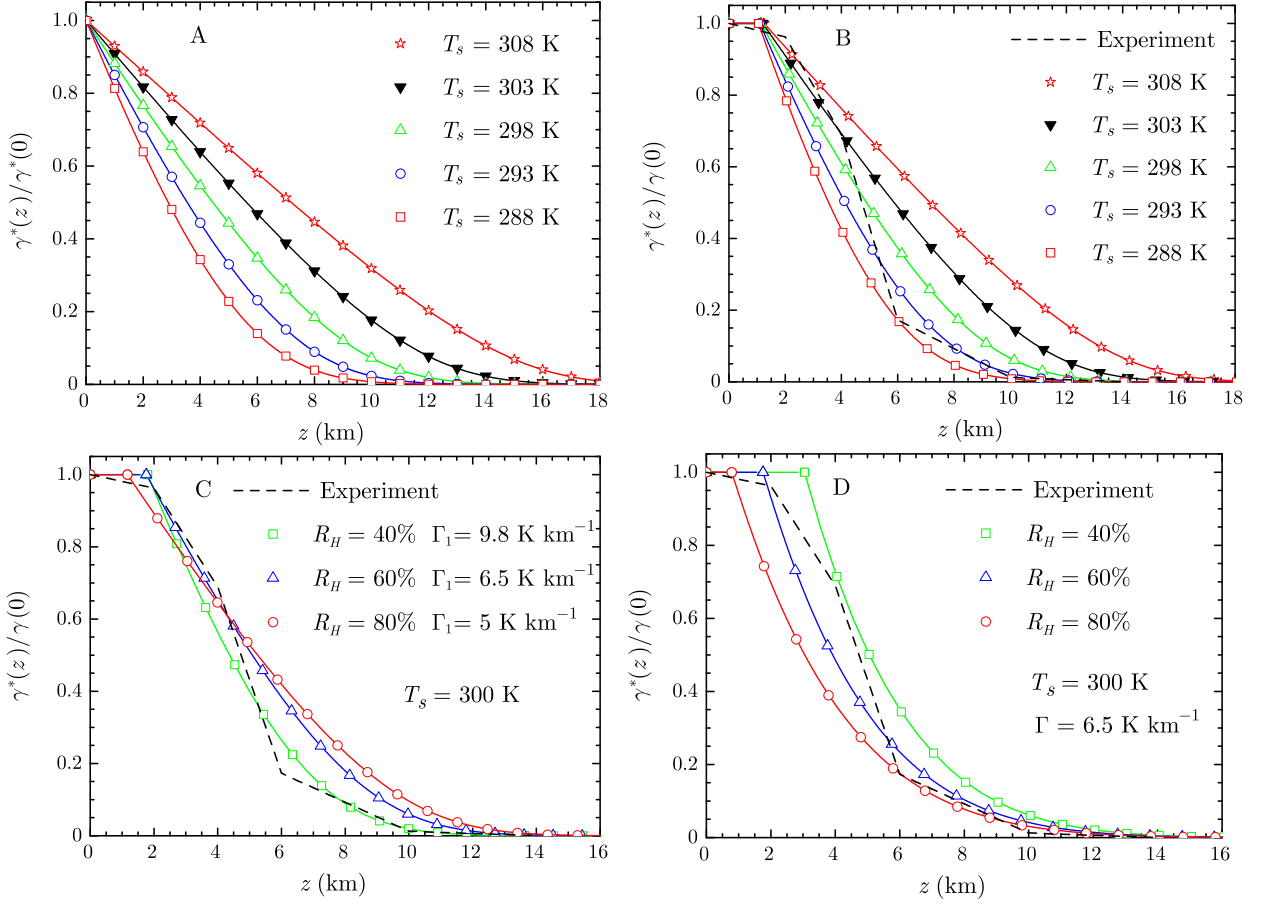


FIG. 2. Vertical distribution of $\gamma^*(z)/\gamma(0)$ under different atmospheric conditions. Dashed curve denotes the mean observed tropical precipitation $P(z)/P(0)$ from Fig. 2 of Pauluis and Dias (2012).

A: Moist adiabat in a completely saturated atmosphere, $R_H = 100\%$, cf. Fig. 1A.

B: The atmosphere is unsaturated at $z < z_1$ ($R_H = 80\%$, $\Gamma_1 = 5 \text{ K km}^{-1}$) and moist adiabatic at $z \geq z_1$, cf. Fig. 1B.

C: The atmosphere is unsaturated at $z < z_1$ and moist adiabatic at $z \geq z_1$.

D: The atmosphere is unsaturated at $z < z_1$, saturated at $z \geq z_1$ and has a constant temperature lapse rate $\Gamma = 6.5 \text{ K km}^{-1}$ at $z \geq 0$ (cf. curves 7 in Figs. 1B, 1C, and 1D).